Düzce University
Journal of Science & Technology

Research Article

The Production of Hydrochar from Hazelnut Waste and its Use in the Removal of Pb (II) and Cr (III)

Buğra DİKBASAN [a], Sami DURSUN [a,*]

[a]*Department of Metallurgical and Materials Engineering, Konya Technical University, Konya, TÜRKİYE*
** Corresponding author's e-mail address: samidursun@ktun.edu.tr*
DOI: 10.29130/dubited.1584464

ABSTRACT

Heavy metals (HMs) are causing an increasing amount of harm to the environment and living organisms. A variety of studies is being conducted to eliminate or diminish such pollutants. In this study, hydrochar was produced from hazelnut waste (HW), and Pb and Cr ion removal research was conducted with this adsorbent. In this way, both the evaluation of HW was provided and the removal of HMs, which are very harmful for the environment. The structural and morphological properties of the produced hydrochars were characterized by thermogravimetric analysis (TGA), differential scanning calorimetry (DSC), field emission scanning electron microscopy (FE-SEM), Fourier transform infrared (FT-IR), and EDX analyses. The effects of many parameters, such as initial concentration, temperature, adsorbent dosages, contact time, and pH on adsorption were discussed. In the studies executed in different parameter environments, it was determined that hydrochar removed 76% and 67% of Pb and Cr ions, respectively. Also, Langmuir and Freundlich isotherm models, pseudo-first-order and pseudo-second-order kinetic models, and thermodynamic parameters like Gibbs free energy were investigated in order to gain a better understanding of the adsorption system of the generated hydrochar. Furthermore, the hydrochar's reusability as an adsorbent was investigated, and it was demonstrated that the material continued to function effectively even after four cycles.

Keywords: *Adsorption, Hydrochar, Heavy metal, Hazelnut waste*

Fındık Atıklarından Hidrokömür Üretimi ve Pb (II) ve Cr (III) Gideriminde Kullanımı

ÖZ

Ağır metaller çevreye ve canlı organizmalara her geçen gün daha çok zarar vermektedir. Bu tür kirleticileri ortadan kaldırmak veya azaltmak için çok sayıda çalışma yapılmıştır ve yapılmaya da devam etmektedir. Bu çalışmada fındık atığından (HW) hidrokömür üretilmiş ve üretilen bu adsorbanla Pb ve Cr iyonlarının giderim çalışmaları yapılmıştır. Bu şekilde hem HW'nin değerlendirilmesi sağlanmış hem de çevre için çok zararlı olan ağır metallerin giderimi sağlanmıştır. Üretilen hidrokömürlerin yapısal ve morfolojik özellikleri TGA, DSC, FE-SEM, FT-IR ve EDX analizleri ile karakterize edilmiştir. Başlangıç konsantrasyonu, sıcaklık, adsorban dozajları, temas süresi ve pH gibi birçok parametrenin adsorpsiyon üzerindeki etkileri tartışılmıştır. Farklı parametre ortamlarında yapılan çalışmalarda hidrokömürün, Pb ve Cr iyonlarının sırasıyla %76'sını ve %67'sini giderdiği belirlenmiştir. Ayrıca, üretilen hidrokömürün adsorpsiyon sistemini daha iyi anlamak için Langmuir ve Freundlich izoterm modelleri, pseudo-birinci mertebe ve pseudo-ikinci mertebe kinetik modelleri ve Gibbs serbest enerjisi gibi termodinamik parametreler araştırıldı. Ayrıca, hidrokömürün bir adsorban olarak yeniden kullanılabilirliği araştırıldı ve malzemenin dört döngüden sonra bile etkili bir şekilde çalışmaya devam ettiği gözlemlendi.

Anahtar Kelimeler: *Adsorpsiyon, Hidrokarbon, Ağır metal, Fındık atığı*

Received: 14/11/2024, Revised: 10/12/2024, Accepted: 11/12/2024

I. INTRODUCTION

Unconscious consumer society, along with industrial and agricultural operations, are the primary causes of the daily rise in pollution in water resources [1]. The reason for pollution is not only this, but also some natural events can cause this situation [2]. For example, water passing through mineral deposits can produce high concentrations of HMs through erosion or dissolution [3]. Studies have demonstrated that this pollution will worsen daily if preventative measures are not implemented. [4]. To prevent or reduce this pollution, methods including chemical precipitation, ion exchange, membrane filtration, evaporation, and adsorption are used [2, 5]. One of these techniques is adsorption, which uses adsorbents with a high adsorption capacity, a big surface area, and the right pore size [6]. Materials used in the adsorption process include fly ashes, coals, zeolites, metal oxides, and silica gels. Hydrochar utilization has grown significantly in importance recently as a result of the expensive cost of some adsorbent materials [7, 8].

One method for using biomass energy is hydrothermal carbonization, which produces hydrochars [9]. This technology's high conversion efficiency and very moderate reaction conditions provide it significant advantages over other methods like roasting and pyrolysis [10-12]. The hydrochar process is used in several research studies in the literature, and the hydrochars that are produced are used in numerous ways. Yang et al. produced hydrochars from bamboo using the hydrothermal carbonization method. The analyses performed showed that the hydrochar produced from bamboo can improve fuel properties and combustion behavior [13]. Nizamuddin et al. converted palm bark into hydrochar by the hydrothermal carbonization method and examined the chemical, structural, and dielectric properties of the hydrochar [11]. Many hydrochar productions using various wastes, such as corn stalks, fish waste, and pine, can also be given in addition to these studies [14-16].

Türkiye is the country that produces the most hazelnuts in the world and, accordingly, produces the most HW annually [17, 18]. These waste materials are typically used to contaminate or fuel the environment, and there is little evaluation of them. In addition, these biomasses consist mostly of hemicellulose, cellulose, and lignin, which are also cheap. Consequently, it is crucial to turn agricultural wastes like HW into hydrochar. Studies on this topic are growing daily, and these hydrochars play a significant part in eliminating both organic and inorganic contaminants from water. In this way, both local wastes are evaluated, and a method with lower costs compared to other methods is used [19].

In this study, hydrochar production was carried out from agricultural HW, and the obtained hydrochars were used as adsorbents. The chemical, thermal, and morphological properties of the obtained hydrochars were investigated using different analysis techniques such as FT-IR, TGA and DSC analyses, FE-SEM, and elemental analyses. In addition, the effects of contact time, pH, and temperature on the adsorption of Pb and Cr metals by hydrochars were investigated. Additionally, kinetic, adsorption isotherm and thermodynamic research was done to learn more about the adsorption system. Moreover, the reusability of the generated hydrochar was also examined by recycle testing.

II. MATERIAL VE METOD

A. MATERIALS

HW were supplied from the northwestern part of Türkiye (Düzce). The chemicals Lead nitrate ($Pb(NO_3)_2$, purity 99.95%) for Pb ions and Chromium (III) nitrate nonahydrate ($Cr(NO_3)_3.9H_2O$, purity 99%) for Cr ion to be used in adsorption studies were supplied by Sigma-Aldrich.

B. METHOD

HW were supplied from the northwestern part of Türkiye (Düzce). The chemicals $Pb(NO_3)_2$ for Pb ions and $Cr(NO_3)_3.9H_2O$ for Cr ion to be utilized in research on adsorption were supplied by Sigma-Aldrich.

B. 1. Preparation of Metal Ion Solutions

The sources of the tested HMs, $Cr(NO_3)_3.9H_2O$ and $Pb(NO_3)_2$, were dissolved in 1000 mg/L of deionized water to create stock solutions. The appropriate working solution was prepared by diluting this stock solution to appropriate volumes.

B. 2. Preparation of Adsorbent Materials

Tap water was used to clean HWs initially, followed by distilled water. They were then dried for 12 h at 70°C in an oven. The cleaned and dried HW was crushed into smaller particles. These particles were transferred to a hydrothermal reactor with deionized water. Then, the reactor's temperature was adjusted to 220°C and maintained there for 180 min. The reactor was let to cool to room temperature once the reaction ended.

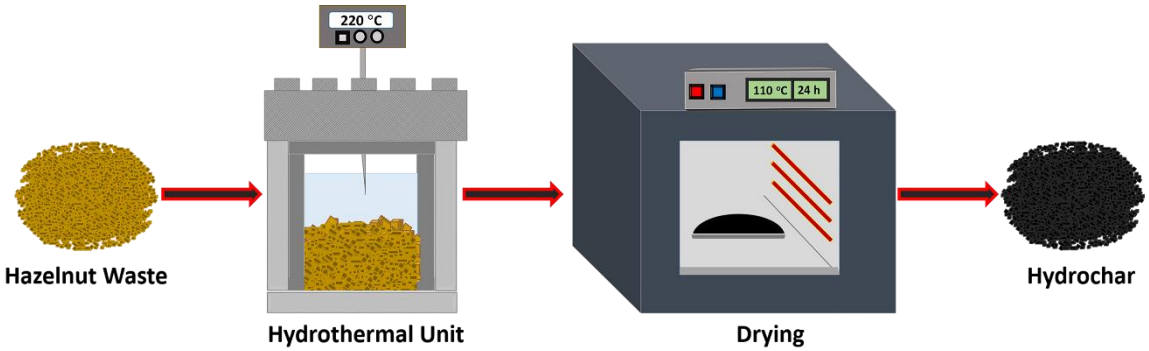

Figure 1. *Schematic diagram of hydrochar production from hazelnut waste*

The obtained hydrochar was filtered with a filter. It was preserved for use in adsorption research after being dried for 24 h at 110°C in an oven. The schematic diagram regarding the production of the hydrochar used as an adsorbent is given in Figure 1.

B. 3. Adsorption Studies of Heavy Metals Ions

In each adsorption study, adsorption experiments were conducted using only one of Pb^{2+} and Cr^{3+}. Experiments with varying parameters were performed to investigate the effects of various environmental conditions on adsorption. In pH effect studies, initial HM concentration was determined as 50 mg/L, hydrochar amount as 50 mg, and shaking time as 240 min. To examine the impact of pH, adsorption tests were realized at pH = 2, 4, 6, 8, and 10. Here, pH adjustments were made using HCl or NaOH solutions. In addition to temperature effect tests conducted at 25°C, 35°C, 45°C, and 55°C, contact time studies were conducted in the range of 0-240 min. In each experiment, 50 mg of hydrochar was put into 100 mL of HM solution (50 mg/L). After each contact time, the concentration was controlled with a UV-visible spectrophotometer (VWR 3100-PC).

C. CHARACTERIZATION

The chemical structures of the hydrochars produced by the hydrothermal system were looked into using FT-IR (Vertex-70 Bruker) spectroscopy. The thermal behavior of the HW and the resulting hydrochar was examined using TGA and DSC studies. The analysis was executed under N_2 atmosphere (25–800

°C temperature range, 20 °C/min heating rate) with a Mettler Toledo brand device. The microstructures and morphologies of the hydrochars used for adsorption prior to and following adsorption studies were examined using a Zeiss Gemini 500 brand FE-SEM. A UV-visible spectrophotometer of the VWR 3100-PC brand was used to control the solution concentration in order to determine the adsorbents' adsorption capability.

D. DATA ANALYSIS

The adsorption capacity of the generated hydrochar and the percentages of HM removal were calculated with the use of Equations 1 and 2.

$$q_e = \frac{C_0 - C_e}{M} \times V \quad (1)$$

$$\%\,Removal = \frac{C_0 - C_e}{C_0} \times 100 \quad (2)$$

C_0 (mg/L) and C_e (mg/L), respectively, represent the starting and equilibrium concentrations of HM ions in the solution. The weight of the adsorbent is represented by M (g), the volume of the solution used in the tests by V (L), and the quantity of HM ions adsorbed by qe (mg/g).
In the study, adsorption isotherm studies were executed to design an optimum adsorption system. Equilibrium isotherm data were assessed through utilization of the most preferred Langmuir and Freundlich adsorption isotherms. Equation 3 represents the Langmuir adsorption isotherm.

$$\frac{C_e}{q_e} = \frac{1}{q_{max} K_L} + \frac{C_e}{q_{max}} \quad (3)$$

In this equation, q_{max} (mg/g) defines the maximum adsorption capacity, while K_L (l/mg) defines the Langmuir constant. The equation of another isotherm, the Freundlich adsorption isotherm, is given in Equation 4.

$$ln\ q_e = ln K_F + \frac{1}{n} ln C_e \quad (4)$$

K_F (mg/g) and n in the equation represent the Freundlich constant and heterogeneity factor.
We investigated the adsorption kinetics of hydrochar using pseudo-first- and second-order kinetic models. Equations 5 and 6 provide the equations for these two models, respectively.

$$ln\ (q_e - q_t) = ln q_e - K_1 t \quad (5)$$

The pseudo-first-order rate constant in this equation is denoted as K_1. q_e and q_t represent the amounts of HMs adsorbed on the adsorbent at equilibrium and at any given period.

$$\frac{t}{q_t} = \frac{1}{K_2 q_e^2} + \frac{t}{q_e} \quad (6)$$

K_2 is the pseudo-second-order rate constant in this equation. The amounts of HMs adsorbed on the adsorbent at any given time are indicated by q_e and q_t, as previously mentioned.
The thermodynamic parameters related to adsorption were determined by the equations given below (Equations 7 and 8). Following the calculation of ΔS^0 and ΔH^0 values from the graph's slope and intercept using the provided data, Eq. 10 was employed to ascertain the Gibbs free energy value.

$$ln K_L = \frac{\Delta S^o}{R} - \frac{\Delta H^o}{RT} \quad (7)$$

$$\Delta G = \Delta H - T\Delta S^o \quad (8)$$

where K_L (mL/g), R and T (K) represent the distribution coefficient, gas constant, and temperature of the solution, respectively.

III. RESULTS AND DISSCUSSION

A. FT-IR ANALYSIS

FT-IR tests were executed to learn more about the chemical makeup of the generated hydrochars and to have an idea about the changes that occurred in the hydrochar after HM adsorption studies. FTIR spectra of HW and hydrochar before hydrochar production are given in Figure 2a. When the spectrum of HW was examined, a peak was observed at 3415 cm^{-1}, and it was determined that this peak belonged to the OH stretching vibration, which is commonly found in the cellulose, lignin, and hemicellulose found in HW [20, 21]. The C-H vibration band describes the peak at 2914 cm^{-1}. The peaks belonging to the C=O vibration and C-O stretching of the carboxyl group are located at 1546 and 1454 cm^{-1}, respectively [22]. The vibration of C-N bonds can be related to the peak at 1247 cm^{-1}. The peaks observed at 1071 and 924 cm^{-1} refer to the C-O bond of alcohols and carboxylic acids, respectively [4].
When the spectrum related to hydrochar is examined, a significant change and peak formation are observed compared to the pre-hydrothermal treatment due to hydrolysis. It is seen that the peak belonging to the O-H band is not in the spectrum belonging to hydrochar due to dehydration. Because dehydration is a reaction that usually occurs after macromolecules are hydrolyzed. As a result of hydrothermal removal of hydrophilic hydroxyl groups, hydrophobicity increases, and the peak that is rarely seen in HW at 1600 cm^{-1} is observed more in the hydrochar spectrum. In addition, dehydration and decarboxylation following hydrolysis fragmentation make the carboxylic acid O-H band at 1305 cm^{-1} more apparent [23]. Additionally, the peaks corresponding to the C=C and C–H bonds forming the hydrochar are present at 1463 cm^{-1} and 832 cm^{-1}, respectively [24].

Figure 2b shows the FT-IR curve with the spectra before and after the Pb and Cr ions were adsorbed. The hydrochar's spectrum is presented once again to highlight the differences between its pre- and post-adsorption Pb and Cr ion spectra. The interaction of the Pb and Cr ions with the hydrochar caused a shift in the peaks' positions. The presence of peaks with very low wave numbers is evidenced by the existence of Pb and Cr-hydrochar bonds [25-27].

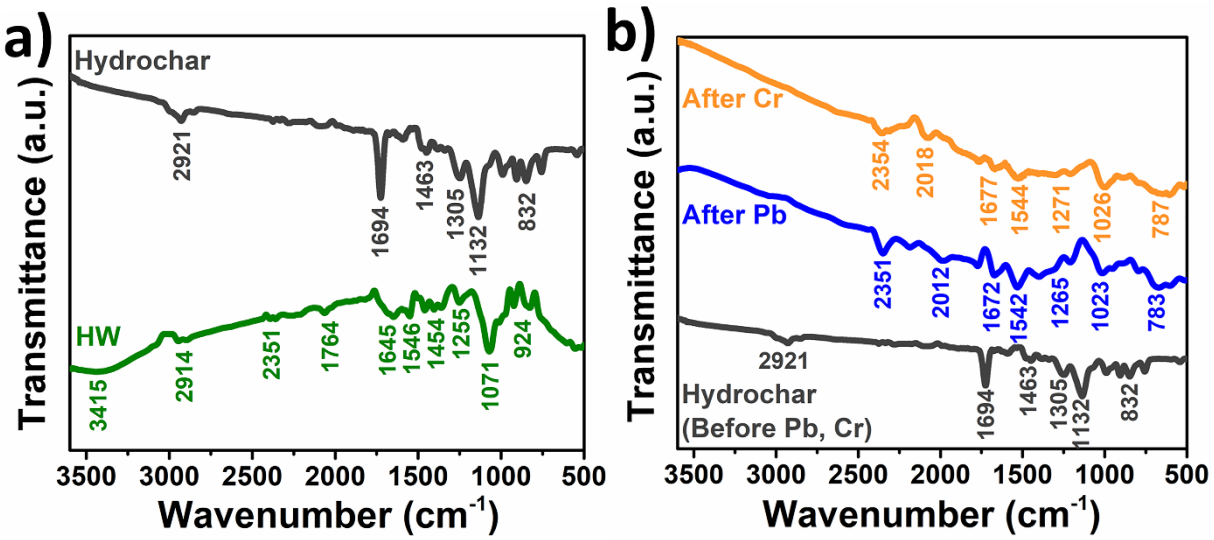

Figure 2. (a) *FT-IR spectra of hazelnut waste and hydrochar* ***(b)*** *before and after adsorption of Pb and Cr ions*

B. TGA AND DSC ANALYSES

The thermal behavior of HW and hydrochar samples resulting from HW was examined using TGA-DSC analyses; the findings are displayed in Figures 3a and b. With a heating rate of 20 °C/min, analyses were fulfilled in the temperature range of 25 to 800 °C. As demonstrated in the HW spectrum in the TGA graph, no appreciable mass decrease was noted in the material up to 200 °C. This shows that the HW has very low internal moisture. The breakdown of cellulose and lignin in the HW's structure explains the 64% mass drop that was observed between 200 and 560 °C [21, 28]. Examining the hydrochar sample reveals that, up to nearly 700 °C, the volume of sample does not diminish. The fact that the weight loss starts around 700 °C indicates that the hydrochar has high thermal stability [29].

When temperatures exceed 700 °C, only a 21% decrease in mass was detected. While the mass loss in the HW sample started at 200 °C, this loss was observed in hydrochars at temperatures above 700 °C. This shows that the thermal stability of the hydrochar is quite high compared to the HW. The other graph supporting this result is the DSC graph, and the HW spectrum in the DSC curve shows that the cellulose and lignin in the HW structure are resistant to degradation and that the material has good thermal stability [30].

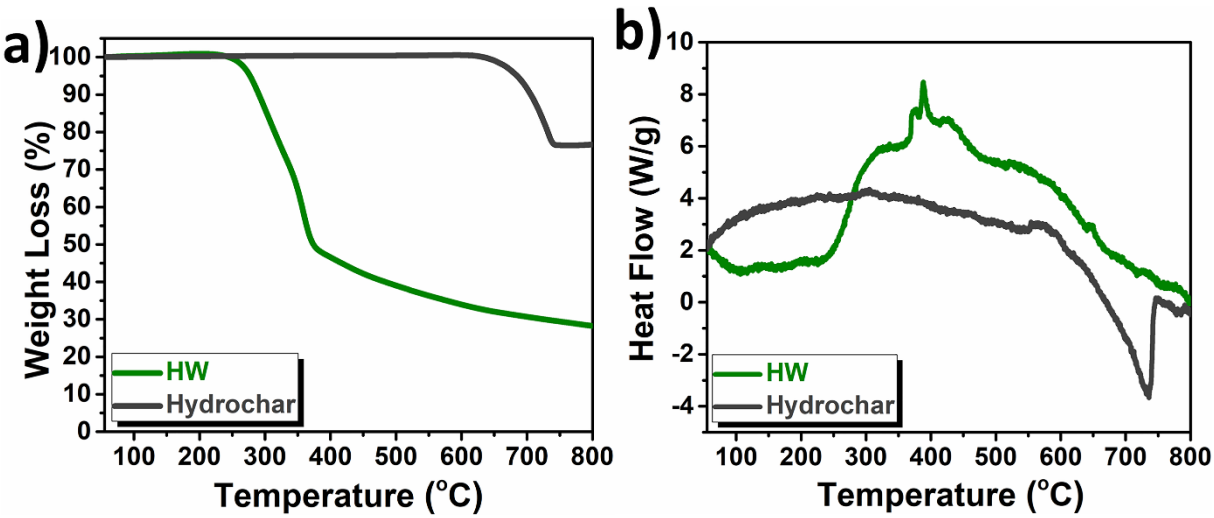

Figure 3. (a) *TGA and,* ***(b)*** *DSC graphs of hazelnut waste and hydrochar*

C. FE-SEM AND EDX ANALYSES BEFORE AND AFTER ADSORPTION

The microstructures and surface morphologies of hydrochars before and after HM adsorption studies were investigated using the FE-SEM imaging technique. The FE-SEM images of hydrochars before adsorption, hydrochars following Pb adsorption, and hydrochars following Cr adsorption are shown in Figures a, c, and e, respectively. The images given in Figures b, d, and f are the EDX and elemental mapping analysis results of hydrochars before adsorption and hydrochars after Pb and Cr adsorption, respectively.

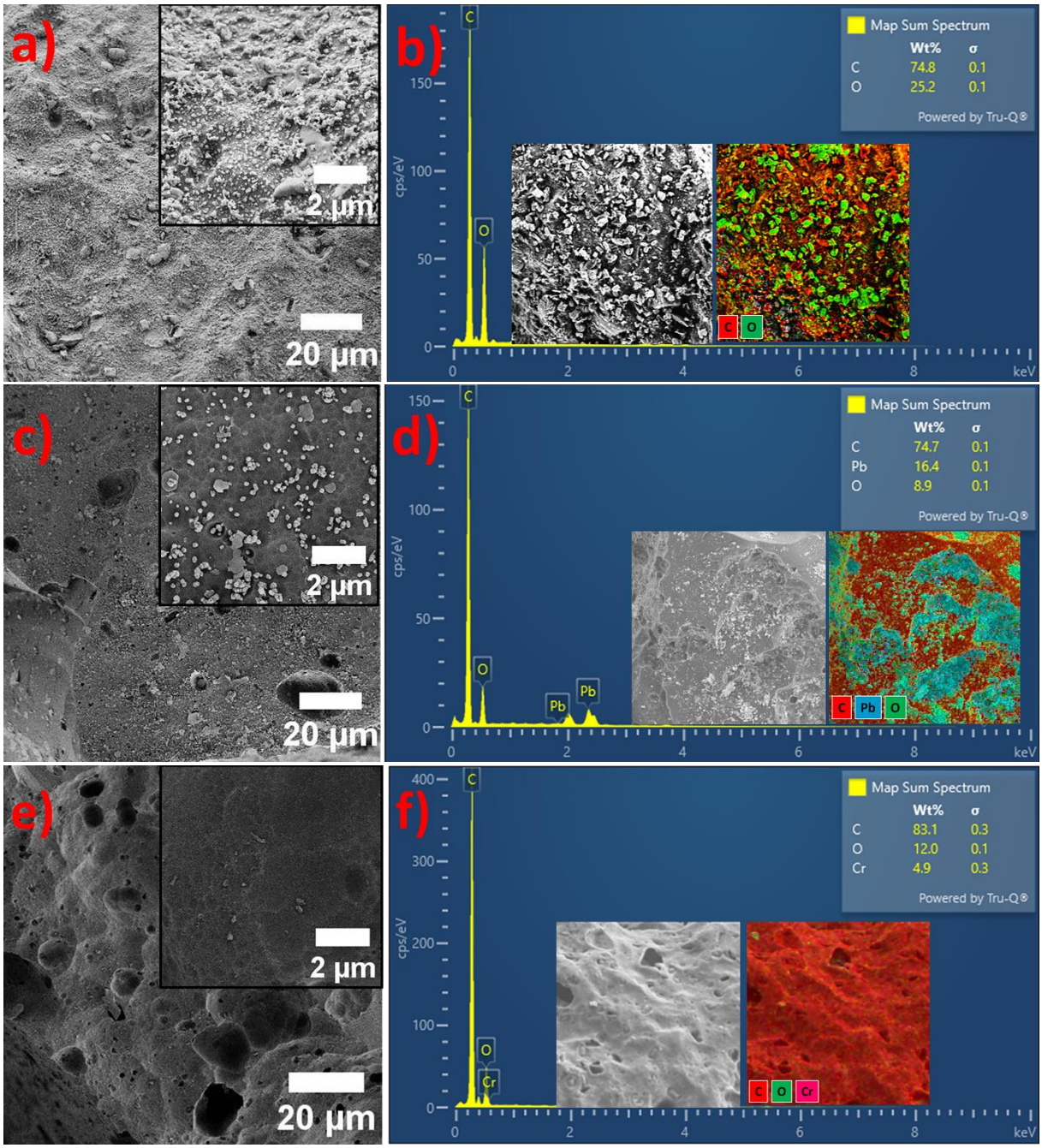

Figure 4. *FE-SEM images of* ***(a)*** *before adsorption,* ***(c)*** *after Pb and* ***(e)*** *Cr adsorption and EDX and elemental mapping analyses of* ***(b)*** *before adsorption,* ***(d)*** *after Pb and,* ***(f)*** *Cr adsorption*

In order to better understand this situation, both before and after adsorption, EDX and elemental analysis measurements were performed. These analyses show that HM were successfully adsorbed by the hydrochar. While only C and O elements are observed in the elemental analysis graph given in Figure 4b, in addition to these, Pb is clearly observed in Figure 4d and Cr is clearly observed in Figure 4f. In addition to these results, elemental mapping measurements also support this result. When the other mapping images are examined compared to the mapping belonging to the hydrochar, the presence of Pb in Figure 4d and Cr in Figure 4f is clearly seen.

D. HEAVY METAL ADSORPTION STUDIES

The initial pH of the medium is very important for the adsorption process. Considering this situation, the effect of pH on Pb and Cr removal was examined and given in Figure 5a. As the pH rose from 2 to 10, it was found in the trials that the elimination of Pb and Cr both reduced. The impact of pH on the interaction between HM ions and hydrochar surface charges describes this circumstance. According to the research, HW biocarbon's zeta potential was 3.81 [32]. According to a different study, the forms of Cr (VI) ions vary depending on the pH of the solution; at pH values below 6.1, $HCrO_4$ is the predominant form of Cr (VI) [33]. The removal of HMs is further promoted at low pH levels by the electrostatic interaction between the positively charged hydrochar and the negatively charged Cr (VI) ions. Furthermore, in an alkaline environment, OH competition might also stop Pb and Cr ions from migrating to the hydrochar surface, which might diminish the effectiveness of HM removal at higher pH levels [34].

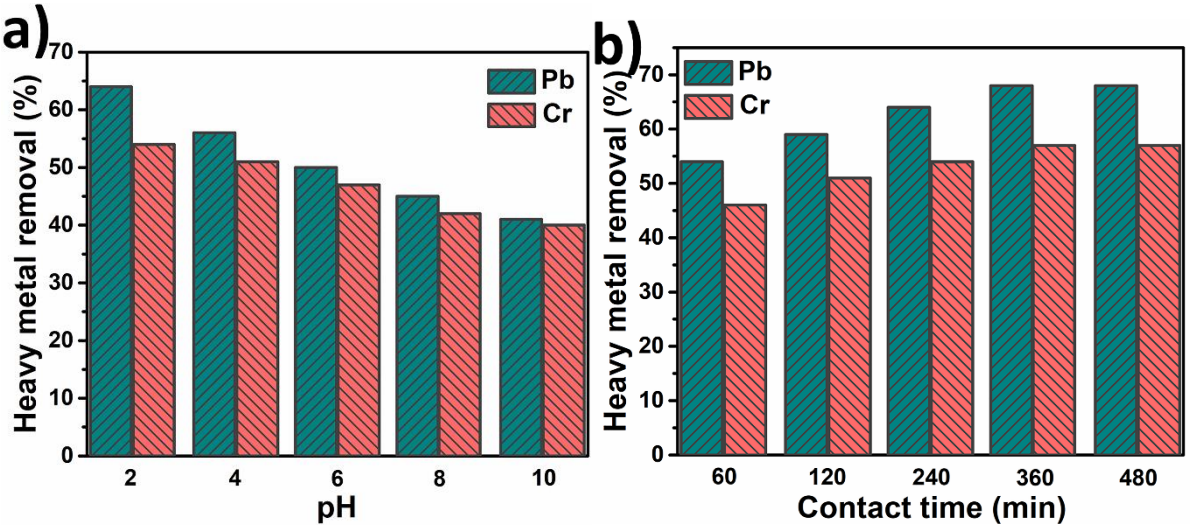

Figure 5. *Effect of* ***(a)*** *initial pH and,* ***(b)*** *adsorption time on heavy metal removal*

Since another important parameter in adsorption is the contact time, studies on the contact time were conducted, and the results are presented in Figure 5b. Although HM ion removal was fast at first, it partially decreased as time progressed. While an increase in removal efficiency was observed up to 360 min, it was determined that the system reached equilibrium at the 360th min. After equilibrium, the adsorption process was continued for another 120 min, but no change was observed in HM removal. This circumstance can be ascribed to the reality that first there were a lot of active sites needed for adsorption on the adsorbent surface, but over time, the number of binding sites on the surface decreased, and after equilibrium, the adsorbent surface's active sites were saturated [35].

Adsorbent dosage and HM initial concentration are the other two parameters affecting the adsorption capacity. Adsorbents of various weights were first added, the medium's pH was brought down to 2, and 240 min of HM removal experiments were conducted. The results are shown in Figure 6a. The graph demonstrates that as the amount of adsorbent grows, so does the effectiveness of HM removal. In the

studies conducted using 20 mg hydrochar, 44% Pb and 40% Cr ions were removed, respectively, while this value reached 64% and 54% in the use of 50 mg hydrochar.

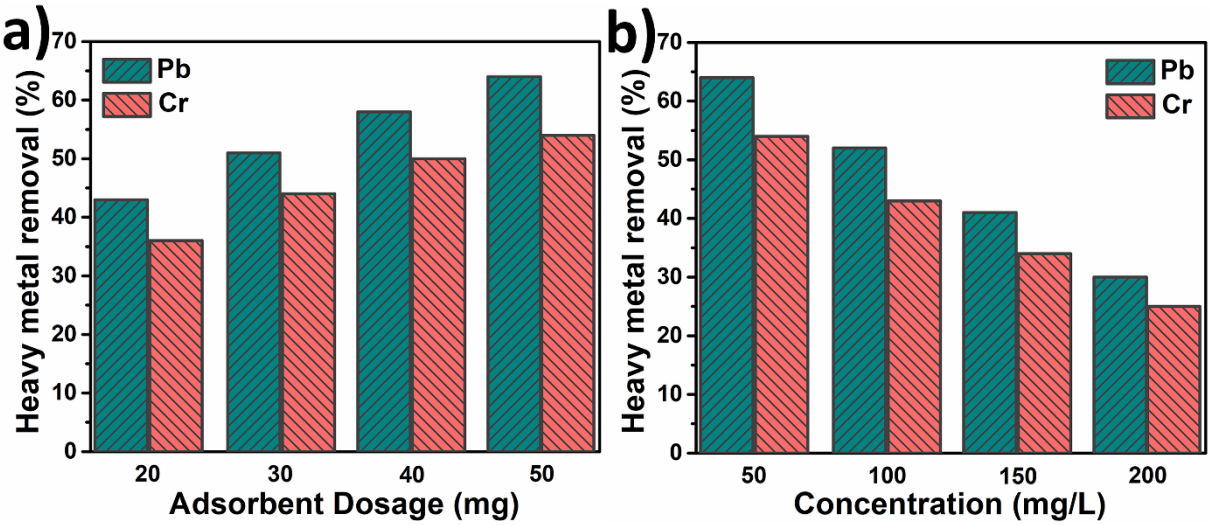

Figure 6. *Effect of* ***(a)*** *adsorbent dosage and,* ***(b)*** *heavy metal initial concentration on heavy metal removal*

The impact of the starting concentration on HM removal was examined using Pb and Cr ions at varying concentrations. These studies were carried out using 50 mg of adsorbent. The graph showing the change in HM removal percentage with HM concentration is given in Figure 6b. According to what the graph indicates, increasing both Pb and Cr concentrations causes a decrease in the removal values of these metals. When Pb and Cr with 50 mg/L concentration are used, the %removal value is 64% and 54%, respectively, while when Pb and Cr with 200 mg/L concentration are used, this value decreases to 30% and 26%. This circumstance results from metal ions' increased ability to engage with the adsorbent's binding sites at low concentrations. However, as the concentration of these HM ions increases, the necessary active sites for adsorption begin to saturate, and the adsorbent cannot remove more HMs [21].

When it comes to adsorption capacity, the effect of both adsorbent dosage and HM initial concentration on metal removal efficiency can generally be related to the active surface area. When the adsorbent dosage is high, there will be more active areas, but since there will not be enough HM, there may not be enough interaction. This causes a decrease in adsorption capacity. The temperature parameter is very important for the removal of HMs. Thereby, the effect of temperature on adsorption was looked into in this phase of the study. Figure 7a presents the study's findings. According to the outcomes, an increase in the removal of both Pb and Cr was detected as the temperature increased. While 64% and 54% of Pb and Cr were removed in the adsorption experiments executed at room temperature, these values were determined to be 75% and 66% in the experiments executed at 55 ºC. The increase in HM removal as the temperature increased means that the process was chemical. The increase in temperature decreased the activation energy that had to be overcome for adsorption to occur and increased the exchange between HM ions and the hydrochar adsorbent [36]. Furthermore, an endothermic adsorption process is indicated by the rise in adsorption capacity with temperature. The studies and results related to the effect of temperature will be utilized in the section on the investigation of thermodynamic properties.

It is critical that materials employed as adsorbents be reusable. For this reason, reusability tests are generally performed, and information can be obtained about how suitable the material used is for use as an adsorbent. Figure 7b displays the findings from the test of the adsorbent's reusability in this study part. Within the parameters of this experiment, four cycles were conducted. After the second, third, and fourth cycles, a decrease of 6.2, 7.0, and 5.3% was observed in HM removal, respectively. According to these findings, the adsorbent continues to play a significant role in the removal of HMs even after four cycles.

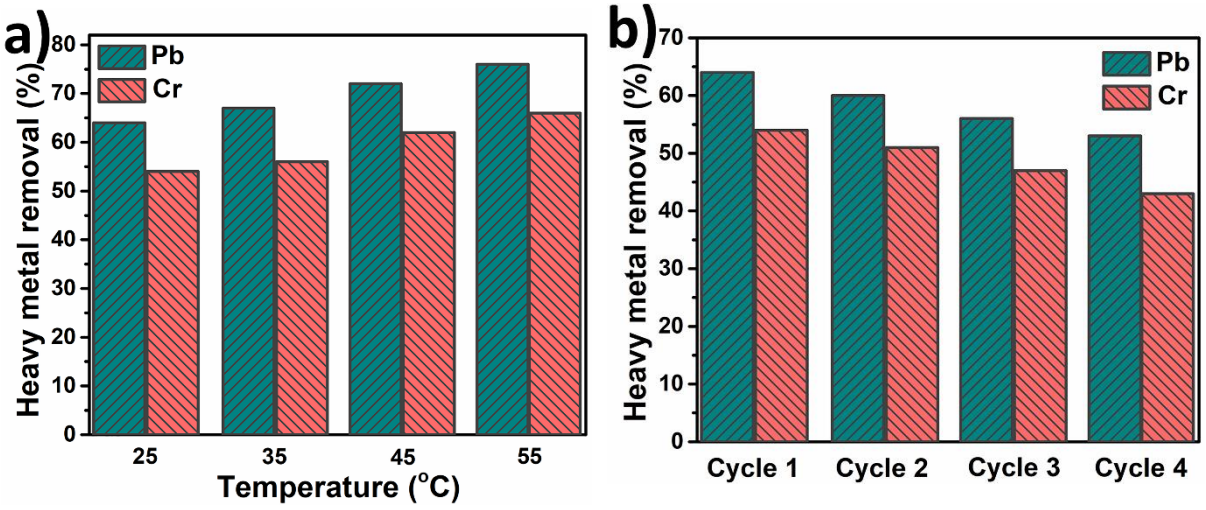

Figure 7. (a) *Effect of temperature on heavy metal removal and* ***(b)*** *hydrochar reusability studies*

E. ADSORPTION ISOTHERM, KINETIC AND THERMODYNAMIC STUDIES

In this section of the research, the isotherm, kinetics and thermodynamics of adsorption are discussed respectively.

E. 1. Adsorption Isotherms

First, the adsorption isotherm is focused on to determine adsorption efficiency. For this purpose, Langmuir and Freundlich isotherms, which come to mind first when the adsorption isotherm is mentioned, were used. To briefly mention both isotherms, the Langmuir isotherm mentions that molecules attached to the surface are attached in a single layer, while the Freundlich isotherm mentions multilayer heterogeneous surfaces [37].

Table 1. *Langmuir and Freundlich isotherm constants.*

	Langmuir			***Freundlich***		
	q_{max} *(mg/g)*	K_1	R^2	K_f *(mg/g)*	***n***	R^2
Pb	*39.308*	*0.038*	*0.997*	*6.121*	*2.833*	*0.962*
Cr	*35.198*	*0.027*	*0.999*	*4.152*	*2.487*	*0.976*

In this section, measurements were first executed using different concentrations of each metal ion for both Pb and Cr (Figure 6b). 100 mL of medium solution, 50 mg of adsorbent, and pH = 2 are the other parameters in the experiments. The title of data analysis gives a thorough explanation of the equations utilized in the computations. Table 1 displays the findings of the computations performed on the experimental data. In the study executed in the presence of Pb ions, the R_2 (correlation coefficients) values of Langmuir and Freundlich isotherms were established as 0.997 and 0.962, respectively. In the presence of Cr ions, these values for the Langmuir and Freundlich isotherms were 0.999 and 0.976, respectively. It is clear that the Langmuir isotherm model has a higher correlation coefficient compared to the Freundlich isotherm model for both HMs. This result shows that the active sites of the hydrochar with equal affinity share the metal ions and that single-layer adsorption is active. In addition, when the calculated n values in the adsorption of both metals are examined, the results being between 1 and 10 indicate that these metals have undergone a suitable adsorption process [38].

E. 2. Kinetic Studies

Adsorption kinetic studies were executed to get an idea about the adsorption mechanism. The kinetic experiments were conducted using pseudo-first- and pseudo-second-order kinetic models. The equations related to both models are given in detail in the data analysis section. Table 2 presents the outcomes derived from the equations utilizing the experimental data. The table shows that when Pb metal is present, the pseudo-second order kinetic model's correlation value (0.997) is higher than the pseudo-first order kinetic model's correlation value (0.915) and approaches 1. The same remains true for Cr (the pseudo-first order kinetic model's correlation value is 0.909, and the pseudo-second order kinetic model's correlation value is 0.998). These findings indicate that the pseudo-second-order kinetic model may account for the adsorption of both metal ions with hydrochars [39].

Table 2. *Adsorption rate constants of pseudo- first-order and second-order kinetic model.*

	Pseudo-first-order			**Pseudo-second-order**		
	$\mathbf{K_1}$ *(1/min)*	$\mathbf{q_e}$ *(mg/g)*	$\mathbf{R^2}$	$\mathbf{K_2}$ *(g/mg min)*	$\mathbf{q_e}$ *(mg/g)*	$\mathbf{R^2}$
Pb	-0.00027	78.671	0.915	0.00113	69.444	0.997
Cr	-0.00031	65.578	0.909	0.00158	58.139	0.998

E. 3. Thermodynamic Study

Thermodynamic parameters also provide ideas about the adsorption process. The equations required to determine the changes in enthalpy, Gibbs free energy, and entropy, which are among these parameters, are provided under the heading "Data Analysis". The graph in Figure 7a was used to determine the thermodynamic parameters. The results obtained through the experimental results and equations are listed in Table 3. Because of the investigation into the adsorption of both metal ions, it was determined that ΔG was negative. This shows that adsorption occurred spontaneously. In addition, the decrease in ΔG values as the temperature increased shows that adsorption continued as the temperature increased. It was observed that ΔH was positive in the adsorption of both Pb and Cr ions. This means that the process is endothermic in both metal adsorption [31, 39].

Table 3. *Thermodynamic parameters for heavy metal ions adsorption.*

	Pb			***Cr***		
T *(K)*	ΔH^o *(kJ/mol)*	ΔG^o *(kJ/mol)*	ΔS^o *(kJ/mol)*	ΔH^o *(kJ/mol)*	ΔG^o *(kJ/mol)*	ΔS^o *(kJ/mol)*
298	1.884482	-0.01834	52.27178	1.686733	-0.01532	42.96343
308		-0.03851			-0.03045	
318		-0.66444			-0.51664	
328		-1.25314			-1.16897	

IV. CONCLUSION

Since the material used in the production of adsorbent in this study is obtained from waste, it will both keep the cost of adsorbent production quite low and increase environmental cleaning as it will be used in the removal of heavy metals. Adsorbents were used to remove Pb and Cr metal ions produced using the hydrocarbon production method. First of all, the characterization of the produced hydrocarbons was carried out and as a result of the characterizations, it was seen that hydrochar was successfully produced. The appropriate conditions for adsorption were determined by considering many different parameters, from adsorbent dosage to pH, contact time to HMs concentration. It was determined that the adsorption

efficiency was higher in low pH conditions, and the highest adsorption occurred at pH=2. In the contact time study, it was observed that the adsorption efficiency increased as time passed at the beginning, and the adsorption efficiency was optimum at 360 min. In addition, as the adsorbent dosage increased, there was an increase in the adsorption of heavy metal ions, while the increase in the heavy metal ion concentration used negatively affected the adsorption. Consequently, to the experiments, the adsorption capacity for Pb and Cr ions was determined to be 39.308 and 35.198 mg/g, respectively. To learn more about the adsorption system, the adsorbent's kinetic, isotherm, and thermodynamic features were investigated. First of all, the adsorption isotherm was focused on to determine the adsorption efficiency, and it was determined that Langmuir was the most suitable isotherm model. Adsorption kinetic studies were performed to get an idea about the adsorption mechanism, and it was pointed out that the second-order kinetic model was noted to be more suitable for adsorption. In addition, thermodynamic properties were investigated to gain more information about the process of adsorption and discovered that the Gibbs free energy values of the adsorption studies for both HM ions were negative, meaning that the adsorption tended to occur spontaneously. Furthermore, experiments were conducted on the reusability of the hydrochar adsorbent in the presence of both Pb and Cr ions, and it was noticed that the adsorbent still played an active role even after four cycles. These results showed that the adsorption capacity of the material selected as adsorbent was sufficient compared to similar materials. In addition, as a result of the recycle studies, it was observed that the produced adsorbent material was quite durable and usable.

ACKNOWLEDGEMENTS: The Konya Technical University Scientific Research Projects (BAP) Fund provided funding for this study under grant number 241019045.

V. REFERENCES

[1] V. Parlak, "Classification of Pollution and Their Entry Rotues into Aquatic Ecosystems," in *Aquatic Toxicology in Freshwater: The Multiple Biomarker Approach*: Springer, 2024, pp. 123-137.

[2] M. Zbair, H. A. Ahsaine, Z. Anfar, and A. Slassi, "Carbon microspheres derived from walnut shell: Rapid and remarkable uptake of heavy metal ions, molecular computational study and surface modeling," *Chemosphere*, vol. 231, pp. 140-150, 2019.

[3] P. Quevauviller, O. Thomas, and A. V. Derbeken, *Wastewater quality monitoring and treatment*. Wiley Online Library, 2006.

[4] M. A. Al-Ajji and M. A. Al-Ghouti, "Novel insights into the nanoadsorption mechanisms of crystal violet using nano-hazelnut shell from aqueous solution," *Journal of Water Process Engineering*, vol. 44, p. 102354, 2021.

[5] G. Argun, G. Çalık, and H. K. Alpoğuz, "Cr (VI) Metal Katyonunun Elektromembran Ekstraksiyonu ile Uzaklaştırılması ve Kinetik Olarak İncelenmesi," *Düzce Üniversitesi Bilim ve Teknoloji Dergisi,* vol. 12, no. 3, pp. 1267-1278, 2024.

[6] Y. Altunkaynak, M. Canpolat, and Ö. Yavuz, "Sulu Çözeltilerden Pb^{2+} İyonlarının Uzaklaştırılmasında Atık Portakal Kabuklarının Kullanılması: Kinetik ve Termodinamik Çalışmalar," *Düzce Üniversitesi Bilim ve Teknoloji Dergisi,* vol. 11, no. 2, pp. 1105-1120, 2023.

[7] G. Crini, "Non-conventional low-cost adsorbents for dye removal: a review," *Bioresource technology*, vol. 97, no. 9, pp. 1061-1085, 2006.

[8] F. Fan, Z. Yang, H. Li, Z. Shi, and H. Kan, "Preparation and properties of hydrochars from macadamia nut shell via hydrothermal carbonization," *Royal society open science*, vol. 5, no. 10, p. 181126, 2018.

[9] F. Fan *et al.*, "Preparation and characterization of biochars from waste Camellia oleifera shells by different thermochemical processes," *Energy & Fuels,* vol. 31, no. 8, pp. 8146-8151, 2017.

[10] J. Zhang, J. Liu, and R. Liu, "Effects of pyrolysis temperature and heating time on biochar obtained from the pyrolysis of straw and lignosulfonate," *Bioresource Technology,* vol. 176, pp. 288-291, 2015.

[11] S. Nizamuddin, N. Mubarak, M. Tiripathi, N. Jayakumar, J. Sahu, and P. Ganesan, "Chemical, dielectric and structural characterization of optimized hydrochar produced from hydrothermal carbonization of palm shell," *Fuel,* vol. 163, pp. 88-97, 2016.

[12] T. Wang *et al.*, "Acetic acid and sodium hydroxide-aided hydrothermal carbonization of woody biomass for enhanced pelletization and fuel properties," *Energy & fuels,* vol. 31, no. 11, pp. 12200-12208, 2017.

[13] W. Yang, H. Wang, M. Zhang, J. Zhu, J. Zhou, and S. Wu, "Fuel properties and combustion kinetics of hydrochar prepared by hydrothermal carbonization of bamboo," *Bioresource technology,* vol. 205, pp. 199-204, 2016.

[14] S. Guo, X. Dong, T. Wu, F. Shi, and C. Zhu, "Characteristic evolution of hydrochar from hydrothermal carbonization of corn stalk," *Journal of analytical and applied pyrolysis,* vol. 116, pp. 1-9, 2015.

[15] S. Kannan, Y. Gariepy, and G. V. Raghavan, "Optimization and characterization of hydrochar produced from microwave hydrothermal carbonization of fish waste," *Waste management,* vol. 65, pp. 159-168, 2017.

[16] Q. Wu *et al.*, "Characterization of products from hydrothermal carbonization of pine," *Bioresource technology,* vol. 244, pp. 78-83, 2017.

[17] E. Demirkaya, O. Dal, and A. Yüksel, "Liquefaction of waste hazelnut shell by using sub-and supercritical solvents as a reaction medium," *The Journal of Supercritical Fluids,* vol. 150, pp. 11-20, 2019.

[18] L. Perez-Armada, S. Rivas, B. González, and A. Moure, "Extraction of phenolic compounds from hazelnut shells by green processes," *Journal of Food Engineering,* vol. 255, pp. 1-8, 2019.

[19] H. A. Alhashimi and C. B. Aktas, "Life cycle environmental and economic performance of biochar compared with activated carbon: a meta-analysis," *Resources, Conservation and Recycling,* vol. 118, pp. 13-26, 2017.

[20] T. H. Tran *et al.*, "Adsorption isotherms and kinetic modeling of methylene blue dye onto a carbonaceous hydrochar adsorbent derived from coffee husk waste," *Science of the Total Environment,* vol. 725, p. 138325, 2020.

[21] S. Dursun, "Production of novel hazelnut shell-based semi-IPN biocomposite absorbents and their use in removing heavy metal ions from water," *Environmental Science and Pollution Research,* vol. 30, no. 15, pp. 44276-44291, 2023.

[22] E. Pehlivan, T. Altun, S. Cetin, and M. I. Bhanger, "Lead sorption by waste biomass of hazelnut and almond shell," *Journal of hazardous materials,* vol. 167, no. 1-3, pp. 1203-1208, 2009.

[23] A. Funke and F. Ziegler, "Hydrothermal carbonization of biomass: A summary and discussion of chemical mechanisms for process engineering," *Biofuels, Bioproducts and Biorefining,* vol. 4, no. 2, pp. 160-177, 2010.

[24] M. T. Reza *et al.*, "Hydrothermal carbonization of biomass for energy and crop production," *Appl. Bioenergy,* vol. 1, no. 1, pp. 11-29, 2014.

[25] P. Wang *et al.*, "Synthesis and application of iron and zinc doped biochar for removal of p-nitrophenol in wastewater and assessment of the influence of co-existed Pb (II)," *Applied Surface Science,* vol. 392, pp. 391-401, 2017.

[26] A. Mandal, N. Singh, and T. Purakayastha, "Characterization of pesticide sorption behaviour of slow pyrolysis biochars as low cost adsorbent for atrazine and imidacloprid removal," *Science of the Total Environment,* vol. 577, pp. 376-385, 2017.

[27] D. Kołodyńska, J. Bąk, M. Kozioł, and L. Pylychuk, "Investigations of heavy metal ion sorption using nanocomposites of iron-modified biochar," *Nanoscale Research Letters,* vol. 12, pp. 1-13, 2017.

[28] M. A. Mahmood and S. Ceylan, "Insights into reaction modeling and product characterization of hazelnut shell pyrolysis," *BioEnergy Research,* pp. 1-11, 2021.

[29] L. K. Palniandy, L. W. Yoon, W. Y. Wong, S.-T. Yong, and M. M. Pang, "Application of biochar derived from different types of biomass and treatment methods as a fuel source for direct carbon fuel cells," *Energies,* vol. 12, no. 13, p. 2477, 2019.

[30] H. Siddiqi, M. Bal, U. Kumari, and B. Meikap, "In-depth physiochemical characterization and detailed thermo-kinetic study of biomass wastes to analyze its energy potential," *Renewable Energy,* vol. 148, pp. 756-771, 2020.

[31] N. Kaya and Z. Yildiz Uzun, "Investigation of effectiveness of pyrolysis products on removal of alizarin yellow GG from aqueous solution: a comparative study with commercial activated carbon," *Water Science and Technology,* vol. 81, no. 6, pp. 1191-1208, 2020.

[32] Y. Zhang, Y. Tang, R. Yan, J. Li, C. Li, and S. Liang, "Removal performance and mechanisms of aqueous Cr (VI) by biochar derived from waste hazelnut shell," *Environmental Science and Pollution Research,* vol. 30, no. 43, pp. 97310-97318, 2023.

[33] S. Rha and H. Y. Jo, "Waste foundry dust (WFD) as a reactive material for removing As (III) and Cr (VI) from aqueous solutions," *Journal of hazardous materials,* vol. 412, p. 125290, 2021.

[34] L. Liu, X. Liu, D. Wang, H. Lin, and L. Huang, "Removal and reduction of Cr (VI) in simulated wastewater using magnetic biochar prepared by co-pyrolysis of nano-zero-valent iron and sewage sludge," *Journal of Cleaner Production,* vol. 257, p. 120562, 2020.

[35] M. Changmai, P. Banerjee, K. Nahar, and M. K. Purkait, "A novel adsorbent from carrot, tomato and polyethylene terephthalate waste as a potential adsorbent for Co (II) from aqueous solution: Kinetic and equilibrium studies," *Journal of Environmental Chemical Engineering,* vol. 6, no. 1, pp. 246-257, 2018.

[36] V. Jonasi, K. Matina, and U. Guyo, "Removal of Pb (II) and Cd (II) from aqueous solution using alkaline-modified pumice stone powder (PSP): equilibrium, kinetic, and thermodynamic studies," *Turkish Journal of Chemistry,* vol. 41, no. 5, pp. 748-759, 2017.

[37] K. V. Kumar *et al.*, "Characterization of the adsorption site energies and heterogeneous surfaces of porous materials," *Journal of materials chemistry A,* vol. 7, no. 17, pp. 10104-10137, 2019.

[38] M. B. Gholivand, Y. Yamini, M. Dayeni, S. Seidi, and E. Tahmasebi, "Adsorptive removal of alizarin red-S and alizarin yellow GG from aqueous solutions using polypyrrole-coated magnetic nanoparticles," *Journal of Environmental Chemical Engineering,* vol. 3, no. 1, pp. 529-540, 2015.

[39] G. Torğut and K. Demirelli, "Comparative adsorption of different dyes from aqueous solutions onto polymer prepared by ROP: kinetic, equilibrium and thermodynamic studies," *Arabian Journal for Science and Engineering,* vol. 43, pp. 3503-3514, 2018.